Upwelling of the Cold Slope Water around the Shelf Edge of the East China Sea

Atsuyoshi MANDA, Atsuhiko ISOBE*1, Takeshi MATSUNO*2, In-Seong HAN*3, Kouichiro KAMIO*4, Tetsuo YANAGI*2, Hideaki NISHIDA, Yasuhiro MORII, Nobuhiro YAMAWAKI, Hirhoshi YOSHIMURA, Hisao KANEHARA and Takeshi AOSHIMA

In order to determine the vertical velocity around the shelf edge of the East China Sea, the assimilation of the ADCP (acoustic Doppler current profiler) and CTD (conductivity-temperature-depth profiler) data is performed. The result of the assimilation shows the strong upwelling of about 10^{-2} cm s^{-1} with shoreward motion during the passage of the Kuroshio frontal eddy. The Lagrangian particle tracing experiment is also conducted to examine the movement of the nutrient-rich cold slope water. The result of the experiment indicates that most of the upwelled cold slope water penetrated onto the shelf moves in the deep layer near the bottom, not in the euphotic layer near the sea surface, in contrast to the upwelling induced by the Gulf Stream frontal eddy.

Key Words: Kuroshio, frontal eddy, upwelling, East China Sea

1. Introduction

A warm filament with a cold-core eddy termed "frontal eddy" has been frequently observed in both Kuroshio and Gulf Stream frontal regions[1,2]. The upwelling in frontal eddies can transport nutrients in the cold slope water into the shelf. This transport of new nutrients from the slope provides a major food source for a succession of biological responses[1]. Phytoplankton and bacterioplankton production of the middle and outer southeastern U.S. shelf is controlled principally by the upwelling-intrusion events of the cold slope water associated with the Gulf Stream frontal eddy[3]. Ishizaka[4] developed the physical-biological model for the southeastern U.S. shelf ecosystem and performed the numerical experiments to reproduce the chlorophyll field derived from the Coastal Zone Color Scanner (CZCS) data. He concludes that the upwelling term is essential to reproduce the surface chlorophyll field derived from the CZCS data in his physical-biological model, and that the upwelling is an important process for the vertical transfer of nutrients and other materials. In the shelf region of the East China Sea (ECS), the upwelling due to the Kuroshio frontal eddy is also considered to be an important process to control the primary production[2].

In order to determine the vertical transfer of nutrients from the shelf slope to the shelf, an accurate determination of the vertical velocity is essential. However, it can be hardly obtained directly from observation, since the vertical velocity of ocean currents is much smaller than the accuracy of instruments in general. Estimating the vertical velocity from the horizontal divergence is thought to be an alternative. However, sufficiently accurate determination of the horizontal divergence directly from observation is often impossible because each term of the horizontal divergence is frequently of the same order of magnitude but opposite in sign[5], i.e., the cancellation of the significant digit extremely reduces the accuracy of the horizontal divergence.

In this study, the vertical velocity is obtained as a solution of an inverse problem, i.e., the assimilation of the ADCP (acoustic Doppler current profiler) and CTD (conductivity-temperature-depth profiler) data with a numerical model is performed to estimate the vertical

*1 Interdisciplinary Graduate School of Engineering Sciences, Kyushu University, 6-1 Kasuga-Koen, Kasuga 816-8580, Japan
*2 Research Institute for Applied Mechanics, Kyushu University, 6-1 Kasuga-Koen, Kasuga 816-8580, Japan
*3 Frontier Observational Research System for Global Change, 2-15 Natsusima-cho, Yokosuka, 237-0061, Japan
*4 Tokyo Kyuei Co. Ltd., 6906-10 Shiba Tsurugamaru, Kawaguchi 333-0866, Japan

velocity field in the Kuroshio frontal eddy. Moreover, in order to examine the movement of the cold slope water during the passage of the Kuroshio frontal eddy, the Lagrangian particle tracing experiment is also conducted.

This paper is organized as follows. Results of the field observations are briefly discussed in Section 2. In Section 3, the numerical model used in this study and the method of the assimilation are described. Results of the assimilation are given in Section 4. In Section 5, results of the Lagrangian particle tracing experiment are discussed. Conclusions are given in Section 6.

2. Field Observation

The intensive field observations with the CTD (Mark IIIB, Neil Brown) and the ADCP (RD-SC0150, R/D Instruments) were conducted across the shelf edge of the ECS by the T/V Kakuyo-Maru of Nagasaki University. The lines of the ADCP data-tracks and the CTD observation sites are presented in Fig.1. The ADCP surveys were carried out three times per day along the line AA' during the period of 22 to 26 May 1998 and along the line BB' during the period of 24 to 28 May 1999. The ADCP data were obtained with a four-meter vertical bin resolution and a one-minute sampling interval. The open circles on the lines AA' and BB' show the CTD observation sites in 1998 and 1999, respectively. The CTD casts were carried out at each site once per day. The distance between two adjacent CTD observation sites was five nautical miles (9.26 km). In this section, results of the observations are discussed briefly. Details are given in Manda *et al.*[6].

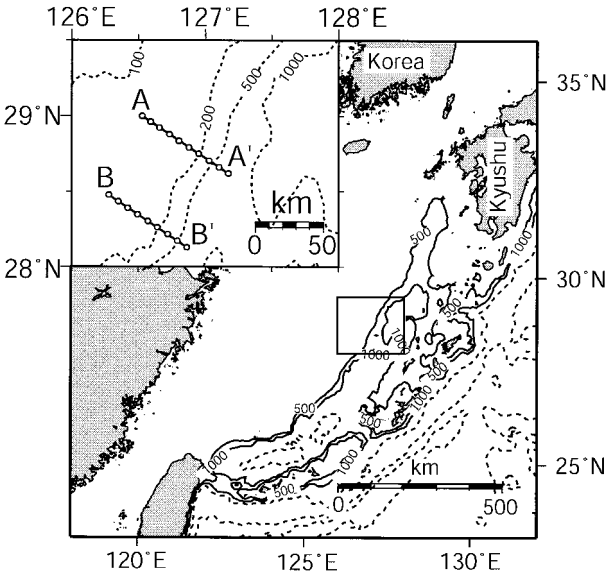

Fig. 1 Map of the East China Sea. The 500-m and 1000-m isobaths are shown as solid contours; dashed contours (unlabelled) are at 1000-m intervals. Inset figure shows the observation area with open circles representing the observation sites of CTD and the lines representing the ADCP-data tracks in 1998 (AA') and 1999 (BB').

2.1. Temperature

Figure 2 shows space-time diagrams of water temperature at a depth of 25 m where the warm filament of Kuroshio frontal eddy was observed Yanagi *et al*[2]. The abscissa shows the distance measured from the most shoreward observation site of the CTD (marked by A in 1998, and B in 1999 in Fig.1) along the obser-

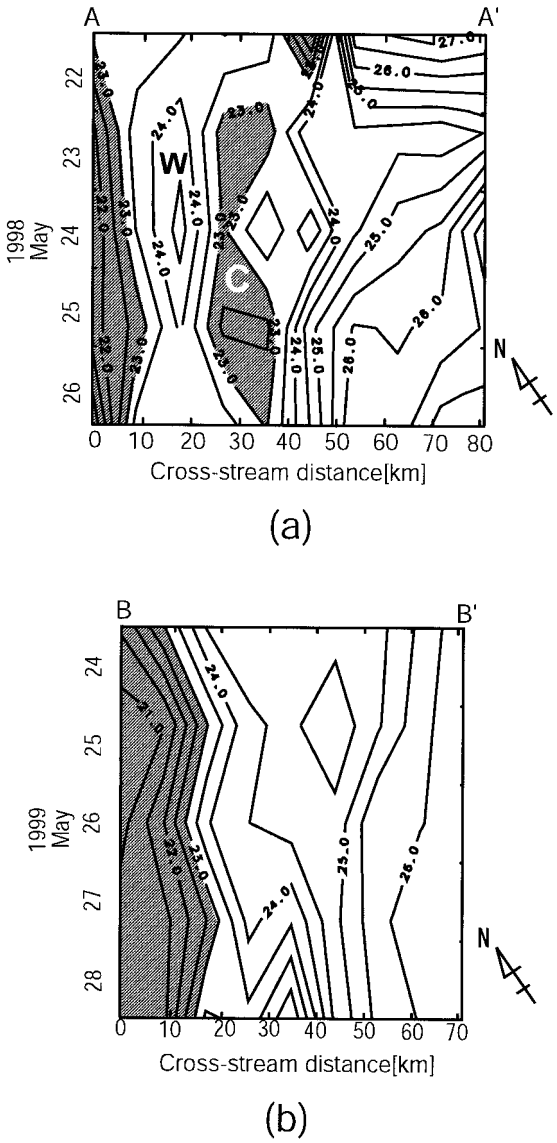

Fig. 2 Space-time diagrams of water temperature (℃) in 1998 (a) and 1999 (b) at a depth of 25m. Shaded areas indicate the areas where temperature is less than 23℃.

vation line, henceforth referred to as the "cross-stream distance." The ordinate shows the date of the observation. In Fig.2(a), we can see the cold water mass and the warm filament indicated by C and W, respectively. Because of the similarity to the Gulf Stream frontal eddy, Yanagi *et al.*[2] referred to this structure as the Kuroshio frontal eddy. On the other hand, the isotherms run relatively parallel to the isobaths in 1999 (Fig.2(b)) compared with those in 1998. This result indicates that the Kuroshio frontal eddy did not appear during the period of the observation in 1999. Figure 3 shows the vertical distributions of temperature. The strong upwelling appeared to occur in 1998 inferred from the elevations of the isotherms. These elevations are not considered to be due to internal tides, since they are not coherent in the cross-stream direction as seen in the tidal currents discussed below. The vertical velocity estimated from the elevations of the isotherms is 30 to 50 m d^{-1}, that is, of order 10^{-2} cm s^{-1}. The estimation will be verified with the assimilation of the ADCP and CTD data with a numerical model in the following sections.

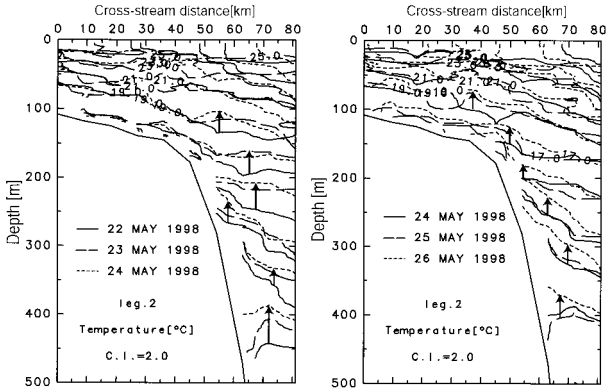

Fig. 3 Vertical distributions of temperature in May 1998.

2.2. Tidal Currents

Tidal currents are strong especially in the shelf region of the ECS[7] and must be removed before the assimilation. We at first describe tidal currents in the study area and then make a comparison of the data before and after the tides are removed.

For the estimation of the tidal currents, the raw records of the ADCP data are divided into 2-day overlapping segments, the lags of which are two hour. Next, the tidal currents of each segment are estimated. Finally, if two or more estimates of the tidal currents are present in different segments at the same time, these estimates are averaged. The method of the estimation of the tidal currents is the same as that by Candela *et al.*[8]. Their method is based on a spatial interpolation scheme, using arbitrary functions, that allow for the temporal variability of tidal currents; it is suitable for the current data obtained from a moving platform such as the ADCP. Details of this method can be found in Candela *et al.*[8]. Candela *et al.*[8] succeeded to resolve the semidiurnal tide from 5-day current measurements along a one-way ship's track in the East China Sea. In the present study, one-minute interval data were used for the harmonic analysis with this method. Thus, we obtain the data with an enough interval to resolve the tidal currents.

Since the observational periods are less than 15 days (the shortest period to resolve the four principal tides (M_2, S_2, K_1 and O_1 tides) in this area), we resolve the semidiurnal and diurnal tides in this study. Figures 4 and 5 show the examples of the calculated tidal ellipses during the periods from 22 to 26 May 1998 (along the line AA') and from 24 to 26 May 1999 (along the line BB'), respectively. These figures indicate the semidiurnal tides are dominated in this area. Moreover, tidal currents seem to be almost barotropic and vertically in phase in the cross-stream direction.

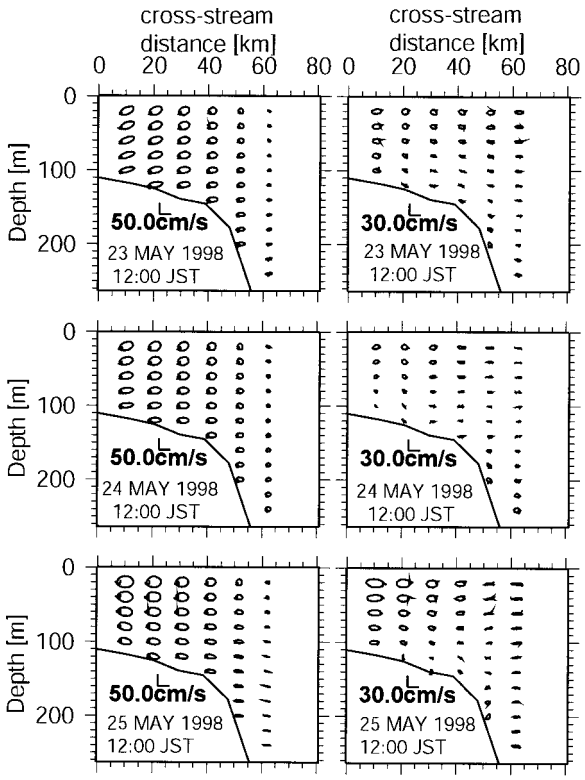

Fig. 4 Examples of the calculated tidal ellipses of semidiurnal (left) and diurnal (right) tides in 1998. Date, month, year, and time in each panel indicate the reference time of each segment for the estimation of the tidal currents.

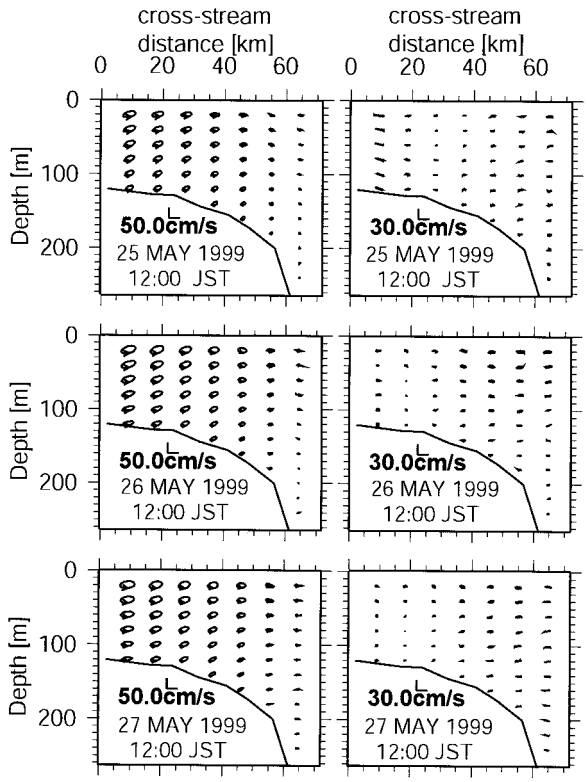

Fig. 5 Same as Fig.4 except for 1999.

Thus, the horizontal distributions of the currents at one depth are presented here. Figures 6 and 7 show space-time diagrams of the raw and de-tided horizontal velocity field at a depth of 25 m during the periods from 22 to 26 1998 and from 24 to 28 May 1999, respectively. In both periods, tidal period fluctuations appeared in the raw records are well removed.

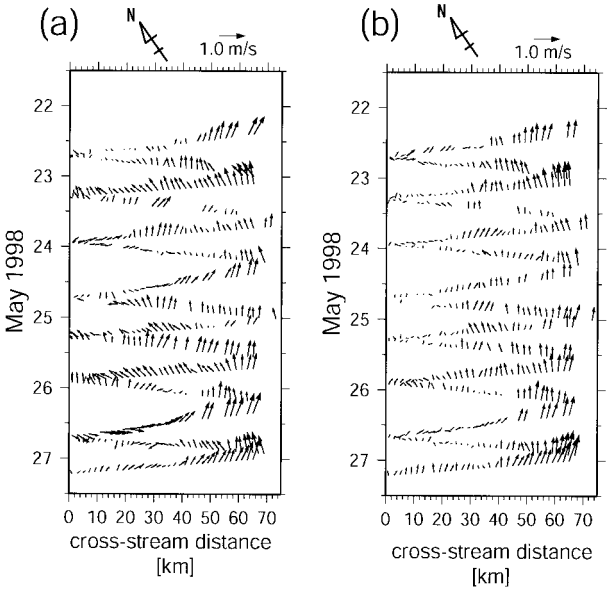

Fig. 6 Space-time diagrams of the raw (a) and the de-tided (b) horizontal velocity at a depth of 25 m in 1998.

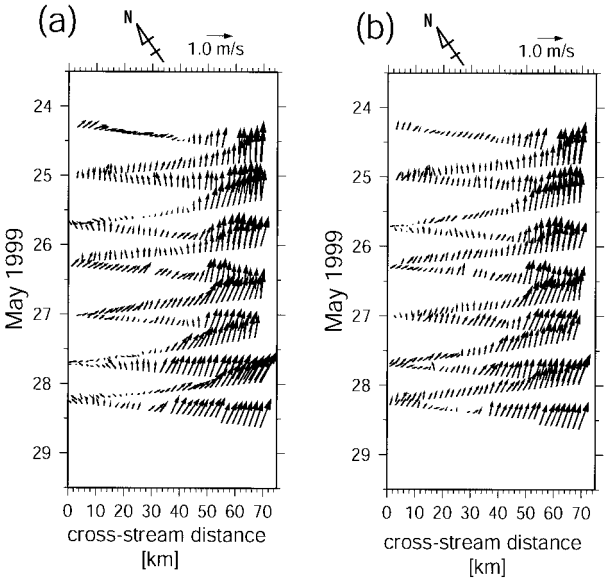

Fig. 7 Same as Fig.6 except for 1999.

3. Estimation of Vertical Velocity

In order to obtain the vertical velocity field in the Kuroshio frontal eddy, the assimilation of the ADCP and CTD data with the numerical model is performed. The fundamental concept of the method used in this study is described in Sarmient and Bryan[9]. In addition to estimating the unknown property not directly measured such as the vertical velocity, the assimilation is expected to reduce the measurement error in the relatively noisy ADCP data so as to satisfy the model dynamics.

3.1. Method

a. Governing Equations

The numerical model used in this study is the three-dimensional primitive equation model on a beta-plane developed by Tabeta[10] under hydrostatic and Boussinesq approximations for an incompressible fluid. The governing equations of the numerical model are modified for the assimilation as follows:

$$\frac{\partial u}{\partial t}+u\frac{\partial u}{\partial x}+v\frac{\partial u}{\partial y}+w\frac{\partial u}{\partial z}-(f_0+\beta_0 y)v$$

$$=-\frac{1}{\rho_0}\frac{\partial p}{\partial x}+A_h\left(\frac{\partial^2 u}{\partial x^2}+\frac{\partial^2 u}{\partial y^2}\right)+A_v\frac{\partial^2 u}{\partial z^2}+\gamma_m(u^*-u), \quad (1)$$

$$\frac{\partial v}{\partial t}+u\frac{\partial v}{\partial x}+v\frac{\partial v}{\partial y}+w\frac{\partial v}{\partial z}+(f_0+\beta_0 y)u$$

$$= -\frac{1}{\rho_0}\frac{\partial p}{\partial y} + A_h\left(\frac{\partial^2 v}{\partial x^2} + \frac{\partial^2 v}{\partial y^2}\right) + A_v\frac{\partial^2 v}{\partial z^2} + \gamma_m(v^* - v), \quad (2)$$

$$0 = -\frac{1}{\rho}\frac{\partial p}{\partial z} - g, \quad (3)$$

$$\frac{\partial u}{\partial x} + \frac{\partial v}{\partial y} + \frac{\partial w}{\partial z} = 0, \quad (4)$$

$$\frac{\partial T}{\partial t} + u\frac{\partial T}{\partial x} + v\frac{\partial T}{\partial y} + w\frac{\partial T}{\partial z} = K_h\left(\frac{\partial^2 T}{\partial x^2} + \frac{\partial^2 T}{\partial y^2}\right) + K_v\frac{\partial^2 T}{\partial z^2} + \gamma_t(T^* - T), \quad (5)$$

$$\frac{\partial S}{\partial t} + u\frac{\partial S}{\partial x} + v\frac{\partial S}{\partial y} + w\frac{\partial S}{\partial z} = K_h\left(\frac{\partial^2 S}{\partial x^2} + \frac{\partial^2 S}{\partial y^2}\right) + K_v\frac{\partial^2 S}{\partial z^2} + \gamma_t(S^* - S), \quad (6)$$

$$\rho = \rho(T, S, p), \quad (7)$$

where x, y, and z are right-handed Cartesian coordinates in the cross-stream (positive offshore along the observation line), downstream, and vertical (positive upward) directions, respectively, u, v, and w represent velocity components in x, y, and z directions, respectively, t is temperature, s is salinity, p is pressure, ρ is density. Notations of parameters in Eqs. (1)-(7) are as follows:

- ρ_0 reference density, kg m^{-3}.
- g acceleration due to gravity, m s^{-2}.
- f_0 Coriolis parameter, s^{-1}.
- β_0 beta parameter, m^{-1} s^{-1}.
- A_H horizontal viscosity coefficient, m^2 s^{-1}.
- K_H horizontal diffusivity coefficient, m^2 s^{-1}.
- A_V vertical viscosity coefficient, m^2 s^{-1}.
- K_V vertical diffusivity coefficient, m^2 s^{-1}.
- γ_m damping coefficient for the horizontal components of velocity, d^{-1}.
- γ_t damping coefficient for temperature and Salinity, d^{-1}.

Unless specified otherwise, the parameter values used in the model are listed in Table 1.

The last terms in Eqs. (1), (2), (5), and (6) are correction terms for u, v, T, and S, respectively. We refer to these terms as "γ terms." Values of γ_m and γ_t are discussed in the next section. The space-dependent constants u*, v*, T*, and S* are the input data for the assimilation as described below. Density ρ is a rather complicated function of temperature, salinity, and pressure; it is calculated from Eq. (7) which represents the equation of state described in Gill[11].

Table 1. Parameters for the standard case.

Symbol	Value
ρ_0	1025 kg m^{-3}
g	9.806 m s^{-2}
f_0	6.962×10^{-5} s^{-1} [a], 6.873×10^{-5} s^{-1} [b]
β_0	2.005×10^{-12} $m^{-1}s^{-1}$ [a], 2.012×10^{-12} $m^{-1}s^{-1}$ [b]
A_H	20 m^2 s^{-1}
K_H	20 m^2 s^{-1}
A_V	1.0×10^{-4} m^2 s^{-1}
K_V	1.0×10^{-4} m^2 s^{-1}
γ_t	1 d^{-1}
γ_m	10 d^{-1}

[a] values in 1998.
[b] values in 1999.

b. Input Data

Yanagi *et al.*[2] observed the three-dimensional structure of the Kuroshio frontal eddy along a single transect for 6 days in the same way as in the present study. They assumed that the observed structure of the Kuroshio frontal eddy was advected in a "frozen pattern" along isobaths at a constant phase speed during the short time compared with the period of the frontal meander (about 14 days[12,13]). With this assumption, they translated the temporal variation of the Kuroshio frontal eddy into the spatial structure. As a result, they succeeded in reproducing the observed drifter tracks by using of the Lagrangian particle tracing method with the observed ADCP data. Since the observational period in this study is shorter than that in Yanagi *et al.* (1998), we adopt the same method as in Yanagi *et al.*[2].

Details of the method of Yanagi *et al.*[2] are as follows. The horizontal velocity field is taken as an example to explain the methodology. The same procedure is applied to both temperature and salinity fields. At first, the ordinate in Fig.8(a) is converted to the downstream distance multiplying the phase speed by the time (measured from the end to the start of the observation) as shown in Fig.8(b). In this study, the magnitude of the phase speed is set to 30 cm s^{-1} (26 km d^{-1}) as in Yanagi *et al.*[2]. The validity of this value will be discussed later. Second, the horizontal velocity field is objectively interpolated with the spline technique[14] on a grid of the numerical model as shown in Fig.8(b).

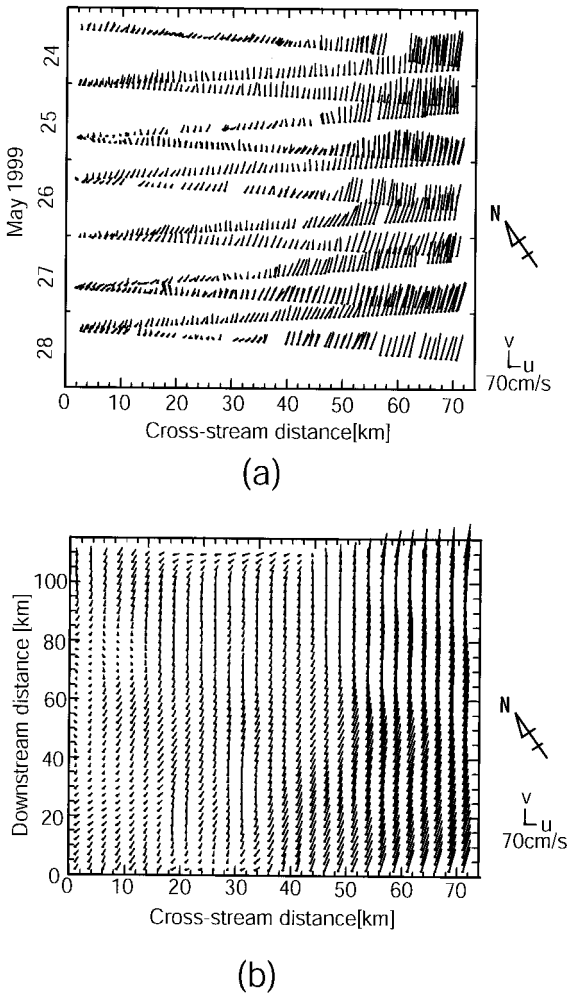

Fig. 8 (a) Space-time diagram of the de-tided horizontal velocity at a depth of 25m.
(b) Interpolated horizontal velocity field for the input data of the robust diagnostic model.

The horizontal velocity field below a depth of 250 m was not obtained by the ADCP. Thus, it is extrapolated through the dynamic calculation using temperature, salinity, and pressure obtained by the CTD with the reference of the de-tided horizontal velocity field at a depth of 250 m.

Since the main purpose of this study is to estimate the order of the vertical velocity of the Kuroshio frontal eddy, we do not deal with the problem arising from the uncertainty of the assumption (e.g., variations of the vertical velocity in the downstream direction).

c. Model Domains and Boundary Conditions

The numerical model domains are schematically shown in Fig.9. Cross-shelf variations of bottom topography are determined from the results of soundings during the CTD observations. The domains are coupled with sponge boundary layers as shown in the shaded regions in Fig.9. We refer to the region inside the sponge boundary layer as the "assimilation region." In the assimilation region, the datasets described above are assimilated. Thus, the point at which both cross-stream and downstream distances are zero corresponds to the point at which x and y equal 40 and 60 km, respectively.

Boundary conditions are described as follows. The periphery of the model domain is treated as an open boundary. On the open boundary, gradients of T, S, u, and v normal to the boundary are set to zero. In the sponge boundary layer, T*, S*, u*, and v* need to be specified. These are obtained by extrapolation with use of the spline technique[14]. In the sponge boundary layer, values of A_h and K_h are ten times as large as those in the assimilation region (those are specified in Table 1). There is no heat and salinity flux through the bottom and the sea surface. Bottom stress (τ_{bx}, τ_{by}) is applied as,

$$(\tau_{bx}, \tau_{by}) = \rho_0 C_d \sqrt{u_b^2 + v_b^2}\,(u_b, v_b), \tag{8}$$

where (u_b, v_b) is the horizontal velocity just above the bottom, C_d $(=2.6\times10^{-3})$ is the drag coefficient. No stress is applied on the free surface.

d. Numerical Method

The equations (1)-(8) are differenced in the rectangular Arakawa staggered C grid system[15]. Vertical representation of the model is so-called z-coordinate system. Temporal integration is performed by the leap-frog stepping with the intermittent use of the Matsuno or Euler-backward scheme[16].

The horizontal resolution in the finite different model is 2.5 km×2.5 km. The thickness of the upper six layers is 20 m. That in the rest of water column is 30, 50, 50, 70, 90, 90, 150, and 160 m. The time step for temporal integration is 10 s.

e. Initial Conditions

Each experiment begins from a state of rest. Temperature and salinity at an initial state are objectively interpolated as described above.

3.2. Results and Discussion

a. Sensitivity to Parameters

In order to determine the optimal values of the damping coefficients, γ_t and γ_m, sensitivity analyses are conducted using the datasets in 1998. Same values of γ_t and γ_m obtained here are applied to the datesets in 1999. Only one parameter was changed from its standard value in each experiment.

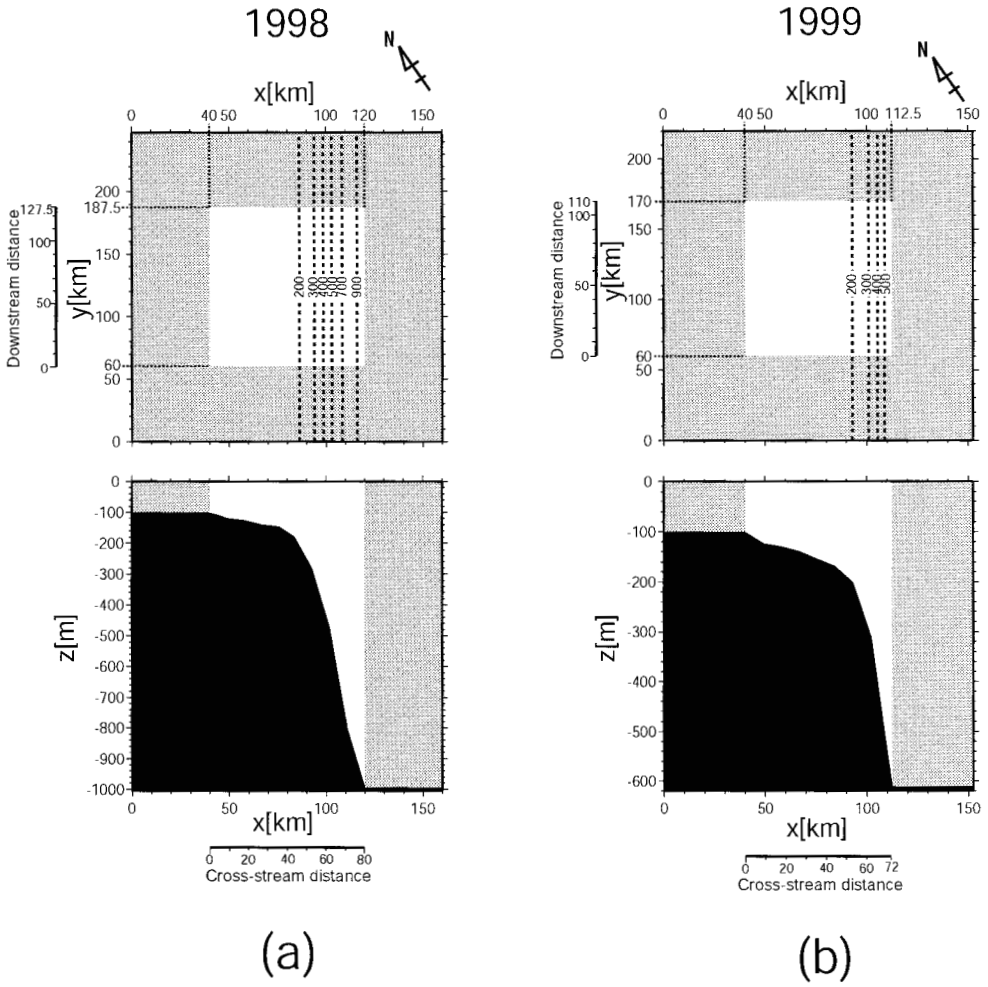

Fig. 9 Model domains in 1998 (a) and 1999 (b). Shaded regions indicate sponge boundary layers. Dashed lines indicate isobaths in meters.

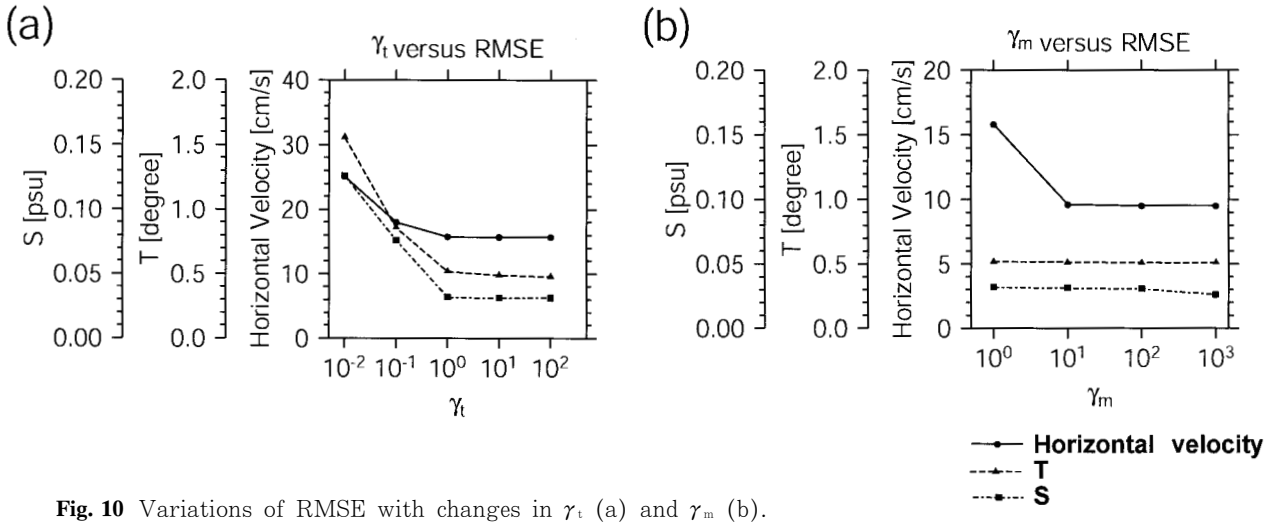

Fig. 10 Variations of RMSE with changes in γ_t (a) and γ_m (b).

The variations of root-mean-square error (RMSE) with changes in γ_t are shown in Fig.10(a). RMSEs of horizontal velocity, temperature and salinity decrease as γ_t increases. However, they do not significantly decrease when γ_t is larger than 1 d^{-1}. Increasing the damping coefficient provides a better fit to the data, but it also indicates a poorer fit to the model. Thus, we adopted 1 d^{-1} for γ_t, since the smaller damping

coefficient is desirable to minimize the distortion of the model.

The variations of RMSE with changes in γ_m are shown in Fig.10(b). The different parameter range for γ_m from that for γ_t is adopted, since changes in γ_m in the same range as that for γ_t result in a poorer fit to the data of the horizontal velocity. This figure shows that RMSEs do not significantly decrease when γ m is larger than 10 d^{-1}. Thus we adopted 10 d^{-1} for γ m for the same reason as γ_t.

The sensitivities to A_H, A_V, K_H, and K_V are also examined. The examinations span a range of parameter variation of two orders of magnitude. The Results show that changes in these parameters do not change RMSEs significantly.

b. Dependence on the Phase Velocity

As mentioned above, we assume that the phase speed of the Kuroshio frontal eddy is 30 cm s^{-1} in the present calculation. In order to examine the effect of the value of the phase speed on the calculated vertical velocity, additional model runs in the cases that the phase speeds are half and twice as that of the present calculation are conducted. The results show that the magnitudes of the calculated vertical velocities in the additional runs are the same order as that in the present calculation. This implies that the variations of the phase speed of the Kuroshio frontal eddy do not significantly affect the estimation of the vertical velocity in the present calculation.

c. Velocity Filed

Figure 11(a) shows the horizontal distribution of the calculated vertical velocity at a depth of 180 m in 1998. The shaded region indicates the upwelling region. We can see the strong upwelling of about 10^{-2} cm s^{-1}

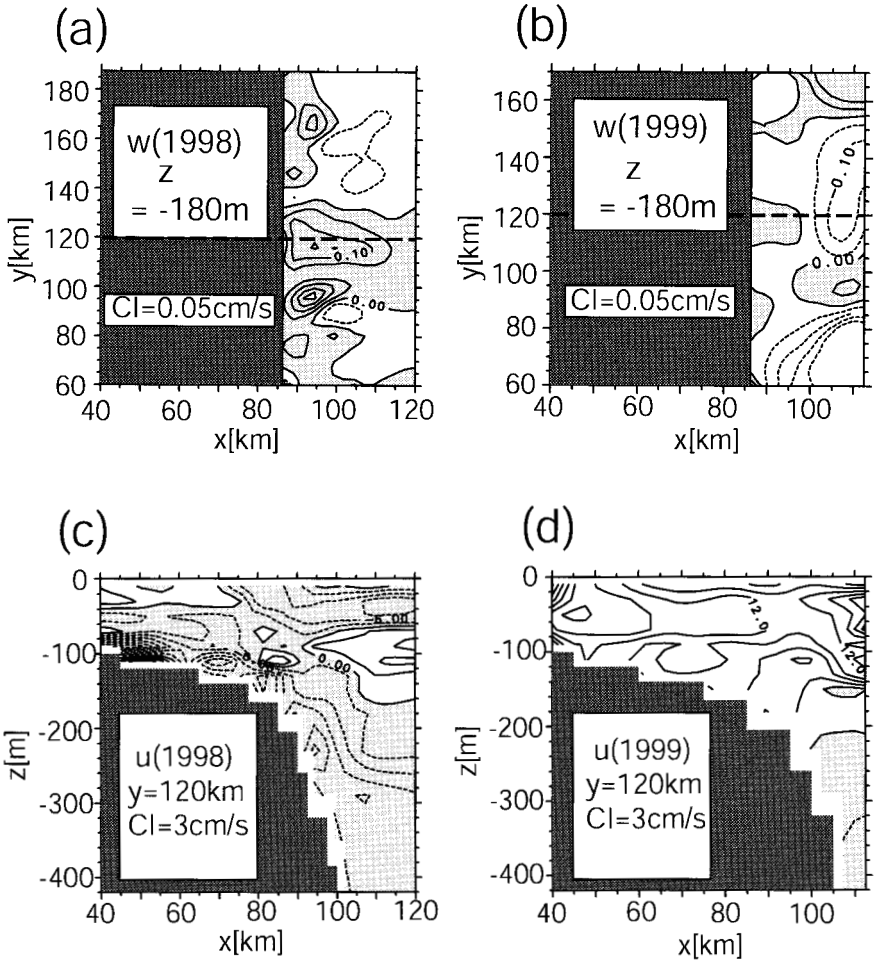

Fig. 11 Horizontal distributions of the vertical velocity (w) at a depth of 180 m in 1998 (a) and 1999 (b). Shaded regions indicate the upward motion. Vertical distributions of the offshore velocity (u) in 1998 (c) and 1999 (d) along the thick dashed lines as shown in (a) and (b), respectively. Shaded regions indicate the shoreward motion.

along the shelf edge. It coincides with the vertical velocity estimated from the elevations of the isotherms as described above. Regions of the relatively large velocity more than 10^{-1} cm s^{-1} are also found, though they are located in limited areas. Figure 11(c) shows the vertical distribution of the calculated offshore velocity (u) along the thick dashed line in Fig.11(a). The shaded region indicates the shoreward motion. The magnitude of the shoreward motion is 5-15 cm s^{-1}. These figures indicate that the upwelled cold slope water moves onto the shelf. On the other hand, in 1999 (Figs 11(b) and 11(d)), the strong upwelling as seen in 1998 is not found. Furthermore, the cross-stream flow is in the offshore direction.

4. Particle Tracing Experiment

In order to examine the primary production in the ECS, it is important to investigate the nutrient transfer from the shelf slope to the shelf. Nutrients in the cold slope water are abundant[1,2]. Thus the strong upwelling accompanied with frontal eddies can transport a large amount of the nutrient-rich cold slope water to the shelf; e.g., the upwelling in the Gulf Stream frontal eddies transports the cold slope water with high nutrient concentrations into the euphotic zone (< 50 m) along the outer shelf[1]. Thus, the upwelled cold slope water is a major source of nutrients for the primary production in the outer southeastern U.S. shelf. The upwelling accompanied with the Kuroshio frontal eddy is also considered to be the important source of nutrients in the ECS[2].

In this section, the Lagrangian particle tracing experiment is conducted to examine the movement of the upwelled cold slope water on the basis of the velocity field obtained in the preceding section.

4.1. Method

The method employed here is the same as described in Imasato *et al.*[17]. The initial distribution of labeled particles is schematically shown in Fig.12. They are placed in the water column where 90 km < x < 120 km, 60 < y < 187.5 km, and -450 m < z < -250 m. The vertical level of the distribution of particles is determined from the result that the relatively high concentration of PO_4-P (> 0.5 μmol l^{-1}) was observed below 250 m deep before the passage of the Kuroshio frontal eddy (Yanagi *et al.*, 1998). Horizontal and vertical distances between two adjacent particles are 1.25 km and 10 m, respectively. The period of particle tracing is 14 days, which is determined from the period of the Kuroshio

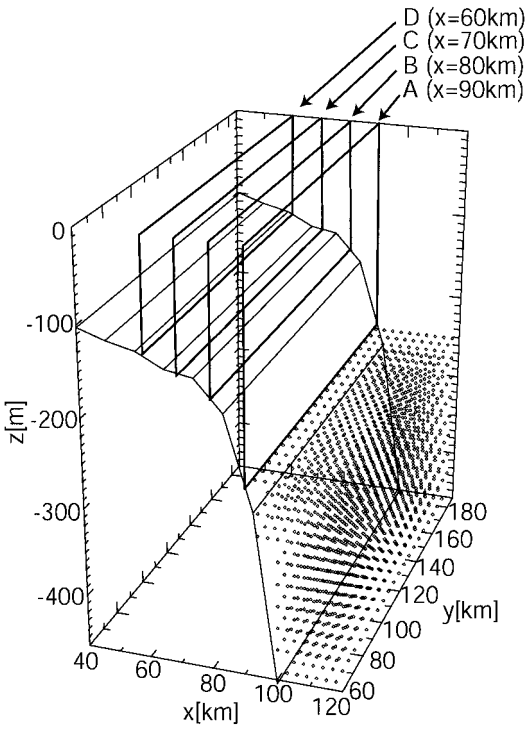

Fig. 12 Schematic view of the initial distribution of particles. Vertical planes A-D indicate the planes to determine the depth at which the particles pass through.

frontal meander[12,13]. The particle that leaves the assimilation region is not traced.

4.2. Results and Discussion

Figure 13 shows the histograms of the relative depth at which the particles pass through each vertical plane as shown in Fig.12. Open circles indicate the points at 50% cumulative frequency counting from the bottom. Half particles pass through the planes below a relative depth of 70-80%. Open squares indicate the points at a depth of 60 m. More than 70% of the particles pass through each plane below a depth of 60 m. Over the outer shelf area near the observation lines in May, the depth of the euphotic layer is roughly estimated to be 50 m. This result indicates that more than 70% of the particles passed below the euphotic layer during the period of the observation in May 1998. Moreover, the observations around the shelf edge of the ECS in 1996 show that the high concentration of PO_4-P appears only below 50 m deep during the passage of the Kuroshio frontal eddy[2]. Thus in contrast to the upwelling accompanied with the Gulf Stream frontal eddy, it is considered that most of the nutrients contained in the upwelled cold slope water in the outer shelf of the ECS are not used in the primary production immediately, but preserved in the deep layer near

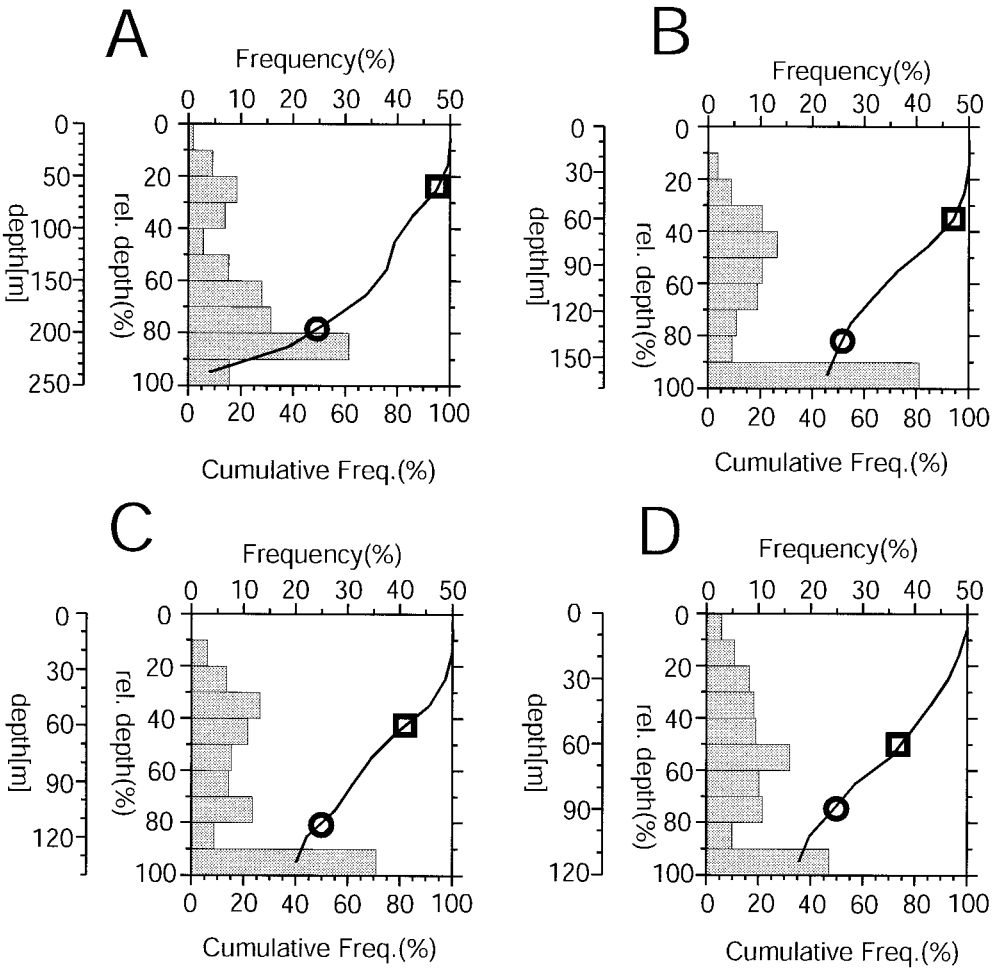

Fig. 12 Histograms of the relative depth at which the particles pass through the vertical planes. See text for details.

the bottom of the shelf. The upwelling velocity due to the Gulf Stream frontal eddy is unknown. However, the above result is probably due to the difference between the depth of the ECS shelf (≅ 160 m) and that of the Georgia continental shelf (≅ 50 m). In order to elucidate the role of the upwelled cold slope water in the primary production in the ECS, the amount of the vertical transfer of the penetrated cold slope water into the euphotic layer and its residence time in that layer need to be investigated. Furthermore, study of the biological processes responding to the nutrient input by the penetrated cold slope water is also needed.

5. Conclusions

The assimilation of the ADCP and CTD data is conducted to determine the vertical velocity of the upwelling during the passage of the Kuroshio frontal eddy. The result of the assimilation shows that the strong upwelling of about 10^{-2} cm s^{-1} occurs, being accompanied with shoreward motion. On the basis of the velocity filed obtained by the assimilation, the Lagrangian particle tracing experiment is also conducted to examine the movement of the cold slope water. The result of the experiment shows that most of the upwelled cold slope water penetrates onto the shelf in the deep layer near the bottom, not in the upper layer near the surface.

Acknowledgements

The authors wish to thank the crew of the T/Vs Nagasaki-Maru and Kakuyou-Maru for their generous assistance in the observations. Thanks are extended to two anonymous reviewers on improving the manuscript. Figures in this paper were produced by the GFD-DENNOU Library and Generic Mapping Tools.

References

1) T. N. Lee, L. P. Atkinson and R. Legeckis: Observation of a Gulf Stream frontal eddy on the

Georgia continental shelf, April 1977, *Deep Sea Res.,* **28A**, 347-378 (1981).

2) T. Yanagi, T. Shimizu, and H.-J. Lie: Detailed structure of the Kuroshio frontal eddy along the shelf edge of the East China Sea, *Cont. Shelf Res.,* **18**, 1039-1056 (1998).

3) T.N. Lee, J. A. Yoder and L.P. Atkinson: Gulf Stream frontal eddy influence on productivity of the southwest U.S. continental shelf, *J. Geophys. Res.,* **96**, 22191-22205 (1991).

4) Ishizaka, J.: Coupling of coastal zone color scanner data to a physical-biological model of the southeastern U.S. continental shelf ecosystem, 2, An Eulerian model, *J. Geophys. Res.*, **95**, 20201-20212 (1990).

5) R. S. Arthur: On the calculation of vertical motion in eastern boundary currents from determination of horizontal motion, *J. Geophys. Res.,* **70**, 2799-2803 (1965).

6) A. Manda, A. Isobe, T. Matsuno, T. Yanagi, I.-S. Han, K. Kamio, H. Nishida, T. Kuno, Y. Morii, N. Yamawaki, H. Yoshimura, H. Kanehara, and T. Aoshima: The results of the intensive ADCP observations of the Kuroshio front in the East China Sea and the detiding procedure, *Eng. Sci. Rep, Kyushu Univ.*, **21**, 343-348 (2000).*

7) X. Guo and T. Yanagi: Three-dimensional structure of tidal current in the East China Sea and the Yellow Sea, *J. Oceanogr.*, **54**, 651-668 (1998).

8) J. Candela, R. C. Beardsley, and R. Limeburner: Separation of tidal and subtidal currents in ship-mounted acoustic Doppler current profiler observations, *J. Geophys. Res.*, **97**, 769-788 (1992).

9) J. L. Sarmient. and K. Bryan: An ocean transport model for the North Atlantic, *J. Geophys. Res.*, 87(C1), 394-408 (1982).

10) S. Tabeta, Numerical simulations of ocean currents in bays by means of multilevel model, Ph. D. thesis, Univ. of Tokyo, Tokyo, Japan (1994).*

11) A.E. Gill,.Atmosphere-Ocean Dynamics, Academic Press, San Diego, Calif., (1982), pp599-600.

12) T. Sugimoto, S. Kimura and K. Miyaji: Meander of the Kuroshio front and current variability in the East China Sea, *J. Oceanogr. Soc. Japan*, **44**, 125-135 (1988).

13) B. Qiu, T. Toda, and N. Imasato: On Kuroshio front fluctuations in the East China Sea using satellite and in situ observational data, *J. Geophys. Res.*, 95(C10), 18, 191-18,204 (1990).

14) Y. Oonishi: Surface interpolation by a spline technique, *J. Oceanogr. Soc. Japan*, **31**, 259-264 (1975).*

15) F. Mesinger and A. Arakawa: Numerical methods used in atmospheric models, GARP Pub. Ser. 17, 1, World Meteorol. Organ., Geneva, 1976, p47.

16) T. Matsuno: Numerical integrations of the primitive equations by a simulated backward difference method, *J. Meteor. Soc. Japan*, **44**, 76-84 (1966).

17) N. Imasato, S. Fujio, Q. Zhang, T. Awaji, and K. Akitomo: Three-dimensional numerical experiments on tidal exchange through a narrow strait in a homogeneous and stratified sea, *J. Oceanogr.*, **50**, 119-139 (1994).

* In Japanese with English summary

東シナ海陸棚縁周辺における陸棚斜面水の湧昇

万田　敦昌，磯辺　篤彦，松野　　健，韓　　仁盛，
神尾光一郎，柳　　哲雄，西田　英明，森井　康宏，
山脇　信博，吉村　　浩，兼原　壽生，青島　　隆

東シナ海陸棚縁周辺で発生する湧昇の鉛直流速を算定するために，ADCP（acoustic Doppler current profiler）とCTD（conductivity-temperature-depth profiler）のデータを数値モデルに同化させた。その結果，外洋から陸棚へと向かう流れに伴って，鉛直流速約10^{-2}cm s^{-1}の強い湧昇が発生していることが明らかになった。この湧昇に伴う，栄養塩に富んだ陸棚斜面水の輸送過程を解明するため，粒子追跡法を用いた数値実験を行った。その結果，陸棚へ湧昇した陸棚斜面水は陸棚の底層に留まり，有光層までは達していないことが明らかになった。